A Low-Loss Linear Analog Phase Modulator for 8415 MHz Transponder Application

N. Mysoor
Spacecraft Telecommunications Equipment Section

A breadboard single-section low-loss analog phase modulator with good thermal stability for a spacecraft transponder application has been analyzed, fabricated, and evaluated. A linear phase shift of 70 degrees with a linearity tolerance of ±7 percent was measured for this modulator from 8257 to 8634 MHz over the temperature range -20°C to 75°C. The measured insertion loss and the static delay variation with temperature were within 2 ±0.3 dB and 0.16 ps/°C, respectively. Four sections will be cascaded to provide the X-band (8415 MHz) phase modulator. The generic modulator design can also be utilized at 7950 to 8075 MHz followed by ×4 multiplication to provide modulation of a Ka-band downlink signal.

I. Introduction

A circulator-coupled reflection phase modulator has been analyzed and investigated to provide the capability to directly modulate an X-band (8415 MHz) downlink carrier for the next generation of spaceborne communications systems. The phase modulator must be capable of large linear phase deviation, low loss, and wideband operation with good thermal stability. In addition, the phase modulator and its driver circuit must be compact and consume low dc power. The design is to provide ±2.5 radians (±143 degrees) of peak phase deviation to accommodate downlink telemetry data and ranging. The tolerance on the phase deviation linearity is ±8 percent. The insertion loss should be less than 10 dB and its variation with phase shift should be within ±0.5 dB. The phase delay variation specifications over the transponder hardware qualification environment, -20 °C to 75 °C, are less than 32 ps/°C for the transponder, and less than 1 ps/°C for the phase modulator. Such stringent specifications make the hardware implementation rather difficult. This investigation will consider the reflection-type phase shifter for the implementation of the hardware. The results extrapolated from analyses and measured performance for a single-section phase modulator with high phase resolution capability are presented in this article. Theoretical analysis of the modulator is presented in Section II. The breadboard modulator configuration and test data are presented in Section III. The conclusions are presented in Section IV.

II. Phase Modulator Analysis

This investigation will consider the circulator-reflection-type phase shifter. A single-stage phase shifter is shown in Fig. 1. Theoretical analysis of the single-stage and multistage phase modulator circuits and their operational amplifier (op-amp) drive circuit are presented in the following subsections.

A. Analysis of a Single-Stage Reflection Phase Modulator

The varactor diode is well suited for the phase modulator application as it can provide rapid phase change with the applied voltage. The circuit model for a packaged diode terminating a transmission line of characteristic impedance Z_o for a reflective phase shifter is shown in Fig. 2. The junction capacitance of abrupt-junction silicon (Si) diodes is modeled as

$$\frac{C_j(V)}{C_o} = \left(1 + \frac{V}{0.8}\right)^{-n}$$

where $C_j(V)$ is the junction capacitance at reverse bias voltage V. C_o is the junction capacitance at $V = 0$.

The diode capacity variation parameter n is the slope of the capacitance-voltage (C-V) curve when plotted on a log-log scaled paper. This slope n is a function of the bias voltage and junction temperature. In the operating bias range of the diode, it can be treated as a constant. The diode capacity parameter n is equal to about 0.5 for practical abrupt-junction silicon diodes. For this analysis, an abrupt-junction silicon diode of capacitance C_j equal to 1 pF at -4 volts bias is considered. Shown in the circuit model of Fig. 2 are the diode junction capacitance, diode leakage resistance (R_s), package inductance (L_p), package capacitance (C_p), lead inductance (L_ℓ), parallel resistance (R_p), and 10-ohm transmission line. In order to obtain large linear phase shift, it is necessary to use a low-impedance transmission line at the diode terminal. The 10-ohm line was selected as it can be realized on a 10-mil-thick alumina substrate. In addition, its line width is not overly wide compared to its length and the diameter of the device package. The package parasitics and the line impedance are optimized to provide linear phase-shift variation with bias voltage. The selected values through analysis and optimization are R_s = 1.5 ohms, L_p = 0.19 nH, C_p = 0.085 pF, L_ℓ = 0.283 nH, and R_p = 100 ohms. The parallel resistance R_p at the diode plane is intentionally added to maintain the insertion loss constant. The calculated phase shift and insertion loss variations with the bias voltage for this model are shown in Fig. 3. The phase shift is linear over the 6- ±5-volt bias range. The linear phase shift over this range is ±65 degrees. The maximum deviation from linearity is within ±6 percent. Any deviation from the optimized circuit component values will result in a reduction in the linear phase-shift range. The circuit component values must be kept within ±10 percent of the optimized values for good results. In particular, the value of package parasitic inductance (L_p) must be within ±5 percent. The insertion loss variation over this voltage range is 2.2 ±0.1 dB. This insertion loss does not include the losses due to the circulator and transmission line matching sections. The estimated total loss including all losses for a single-stage phase shifter is about 3 ±0.1 dB. The insertion loss of a phase modulator must be kept constant with phase shift. The variation of the insertion loss with phase shift causes amplitude modulation (AM) of the RF signal. This AM may get converted to undesirable phase modulation (PM) by subsequent nonlinear operation. The insertion loss can be leveled over the phase-shift range by adding a stabilizing resistor (R_p) in parallel with the varactor diode of each stage (Fig. 2).

B. Analysis of Multistage Reflection Phase Modulator

A series cascade of three circulator-reflection phase shifters will provide ±200 degrees phase shift with ±6 percent error. The estimated total insertion loss, including the input and output isolators, is 10 dB ±0.5 dB. These predictions are based on the analysis of the single stage in the previous section. However, the measured data on the fabricated single-stage reflection phase modulators in Section III projects the use of four stages instead of three stages to meet the linearity requirement. A four-stage circulator-reflection phase modulator, including the modulator drive circuit, is shown in Fig. 4.

C. Phase Modulator Op-Amp Drive Circuit

The functions of the phase modulator drive circuit (Fig. 4) are to sum and amplify the modulation input signals and provide composite drive voltage to the varactor diodes. The modulation input signals include the spacecraft telemetry, ranging, and differential one-way ranging (DOR) signals. The modulation frequency range is from dc to 20 MHz. The selected wideband op-amp for this application is the Comlinear CLC 231. The estimated power dissipation for the drive circuit is 1 watt.

III. Phase Modulator Implementation and Performance

The circuit configuration and measured performance of the breadboard single-stage circulator-reflection phase modulator are given in subsection III-A. Application to Ka-band (31.8 to 32.3 GHz) is also presented in this subsection. The estimated projections for a four-stage phase modulator are presented in subsection III-B.

A. Single-Stage Circulator-Reflection Phase Modulator

1. **Circuit Configuration.** The circuit diagram and a photograph of the phase modulator are shown in Figs. 1 and 5, respectively. The reflection phase shifter configuration [1, 2] makes use of a 50-ohm circulator to provide matched input and output terminals for the phase-shifting diode circuit in the middle path. The circulator used in this investigation is a

broadband 8.4 to 12 GHz circulator (Western Microwave, Inc., 13CX-481, Serial no. 10). The two-way insertion loss of the circulator is 0.6 ±0.1 dB over the operating bandwidth at the nominal temperature of 23 °C. The circuit [Fig. 1] consists of a packaged diode at the end of a 10-ohm line and two quarter-wave matching sections (33.44-ohm and 14.95-ohm sections) to transform 10 ohms at the diode terminals to 50 ohms at the circulator port. The 10-ohm microstrip circuit is etched on a 10-mil-thick Roger 1085 substrate of dielectric constant K = 10.5. The width of the 10-ohm line is 97 mils, which is slightly larger (20 percent) than the diode package diameter of 80 mils. Better than 75 percent size matching between the diode and the line width is necessary in hybrid circuits to reduce insertion loss. The diode's anode is soldered to the ground as shown in Fig. 5. The circuit model for the diode, diode package parasitics, and connecting lead inductance are illustrated in Fig. 2. The junction capacitance of the selected abrupt-junction silicon diode (Alpha Industries, DVH 6733-02 in 168-001 package) is approximately equal to 0.6 pF at −4 volts bias, 0.45 pF at −8 volts bias, and 1.392 pF at 0 volts bias. This results in a diode capacitance ratio of 3:1 from from 0 volts to −8 volts bias range. Such large capacitance variation with bias is necessary to obtain large phase deviation. The series resistance of the diode is 3.6 ohms. The phase deviation characteristics of the circuit are also influenced by the values of package parasitics, interconnection lead inductance, and the length of the 10-ohm line. The typical values of the diode package parasitics supplied by the manufacturer are L_p = 0.5 nH and C_p = 0.18 pF. The inductance of the interconnection lead (L_Q) between the diode package and the 10-ohm line is equal to 0.05 nH. It is difficult to accurately model the package parasitics. The lengths of the interconnection lead (L_Q) and the 10-ohm line can be adjusted to obtain linear phase deviation.

2. Performance of Single-Stage Phase Modulator at 8415 MHz. The measured phase deviation versus bias characteristics for the single-section phase modulator (Fig. 5) are illustrated in Fig. 6. The nominal values of frequency, bias, voltage, and temperature in these measurements are 8415 MHz, 4.5 volts and 23 °C, respectively. The measurement bandwidth range was from 8257 to 8634 MHz. The phase angle was measured at 0 volts bias and the nominal frequency 8415 MHz was used as the reference angle. The measured linear phase deviation for the voltage swing ±3 volts above the nominal bias of 4.5 volts was ±34 degrees with a linearity better than ±7 percent of a best-fitted straight line (BSL). The phase modulator circuit was subjected to temperature tests over the hardware qualification temperature range from −20 °C to 75 °C. As shown in Fig. 7, the overall variation of the static phase with temperature is about 45 degrees with 0.5 degree/°C slope. The calculated static phase delay at 8415 MHz is 0.16 ps/°C. As seen from Fig. 7, the change in the static phase with temperature is not symmetrical about its value at 23 °C. The reason is that the static phase variation of the circulator with temperature is nonlinear. The measured value of the circulator's static phase shift was 2.2 degrees for a change in temperature from 23 °C to 75 °C, and was equal to −17.3 degrees from 23 °C to −20 °C. However, the temperature-induced phase shift for the diode circuit has a linear slope equal to 0.26 degree/°C. Measured insertion loss as a function of varactor bias and temperature are shown in Fig. 8. The RF input power level was equal to 5 dBm at 8415 MHz. The maximum variation of the insertion loss with circulator was found to be 2 ±0.3 dB over the bias levels (4.5 ±3 volts), temperature range (−20 °C to 75 °C), and the RF frequency range (8257 to 8634 MHz). This includes the circulator's two-way insertion loss of 0.6 dB. The diode phase shift and linearity can be calculated if all the circuit component values are known fairly accurately. The values of package parasitics and the diode's junction dynamics are not well known. This results in a discrepancy between the measured and predicted results.

3. Performance of Single-Stage Phase Modulator at 7966 MHz for Ka-Band (31.8 to 32.3 GHz) Application. The single-stage modulator was also evaluated at 7966 MHz to assess its applicability to the Ka-band (31.8 to 32.3 GHz) exciter subsystem. For the Ka-band application, the phase-modulated carrier at 7950 to 8075 MHz is multiplied by four to obtain the signal at Ka-band frequency. The measured phase deviation and insertion loss values are shown in Figs. 9 and 10. The measured bandwidth range about 7966 MHz was from 7807 to 8118 MHz. Figure 9 shows a linear phase shift of ±36 degrees at 7966 MHz with a linearity of ±8 percent over the bias range of 4 volts ±3.5 volts. The insertion loss is flat and is equal to 2 ±0.3 dB. The full phase deviation of ±143 degrees at Ka-band (31.8 GHz) can be obtained by multiplying the output of the single-stage phase modulator (±36 degrees) at 7966 MHz by a ×4 multiplier. The circuit is thus useful for both 8415 MHz (X-band) and 7966 MHz applications (applicable to Ka-band at 4 × 7966 MHz). The measured overall bandwidth of this circuit is 2300 MHz, from 6900 to 9200 MHz.

B. Four-Stage Circulator-Reflection Phase Modulator

Four of the above-mentioned circulator-reflection phase shifter circuits (Fig. 4) in tandem will provide ±143 degrees of linear phase deviation at 8415 MHz, with linearity better than ±8 percent and insertion loss of about 10 ±0.5 dB. The bias range is 4.5 ±3 volts. The estimated size of the 8415 MHz four-stage phase modulator including the wideband op-amp drive circuit is 5.72 by 5.72 by 2.2 cm.

IV. Conclusions

Using a given package-type varactor diode and a circulator, a phase modulator was realized. From 8257 to 8634 MHz, the measured voltage-controlled linear phase deviation, linearity tolerance, and insertion loss were ±34 degrees, ±7 percent, and 2 ±0.3 dB, respectively, over the test temperature range of −20 °C to 75 °C. The static phase delay was found to be 0.16 ps/°C. It is feasible to construct a ±143 degree phase modulator using four such reflector phase-shifting circuits with approximately 10 ±0.5 dB of insertion loss.

Acknowledgments

Acknowledgment is given to the contributions of C. N. Byrom and A. W. Kermode during the course of this work.

References

[1] R. Garver, "360° Varactor Linear Phase Modulator," *IEEE Trans. Microwave Theory Tech.*, vol. MTT-17, pp. 137–147, March 1969.

[2] R. Garver, "Broad-Band Diode Phase Shifters," *IEEE Trans. Microwave Theory Tech.*, vol. MTT-20, pp. 314–323, May 1972.

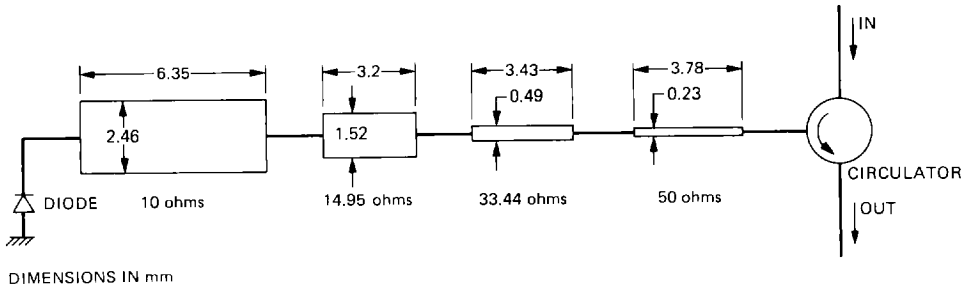

Fig. 1. Phase modulator circuit layout etched on a 0.254-mm-thick soft substrate of dielectric constant K = 10.5.

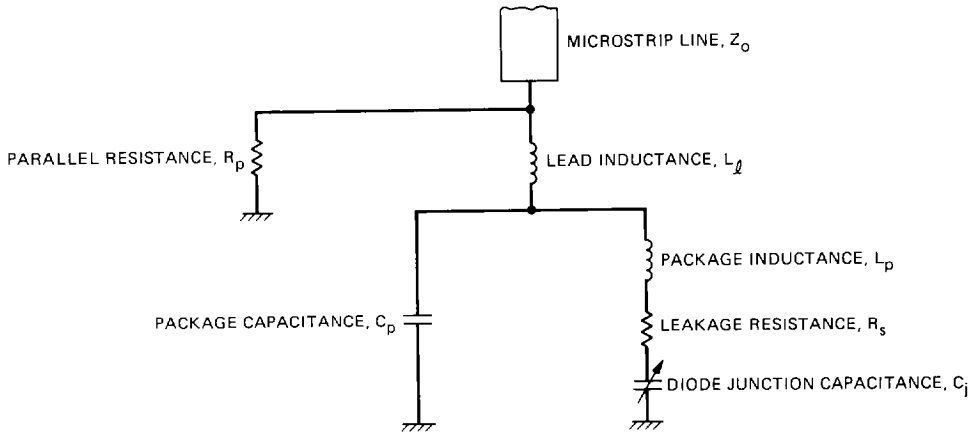

Fig. 2. Phase modulator circuit model.

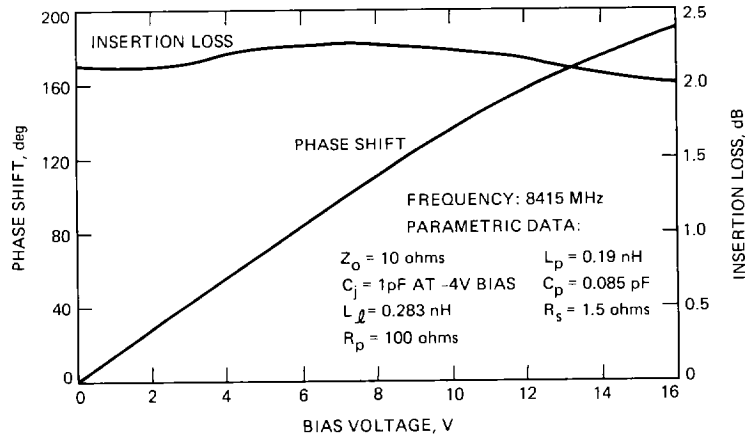

Fig. 3. Calculated phase shift of an optimized single-section phase modulator as a function of dc bias voltage.

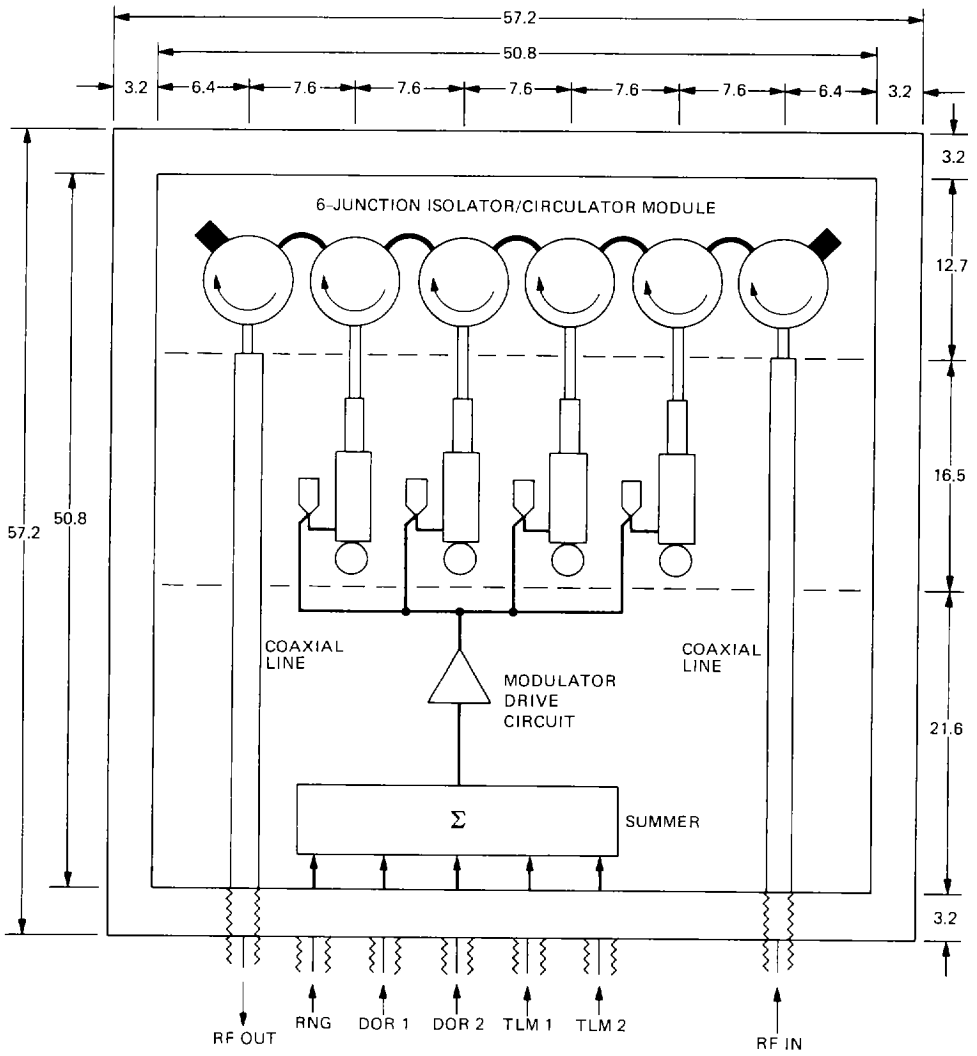

OUTSIDE DIMENSIONS: 57.2 x 57.2 x 21.6
DIMENSIONS IN mm

Fig. 4. Four-stage circulator-reflection phase modulator.

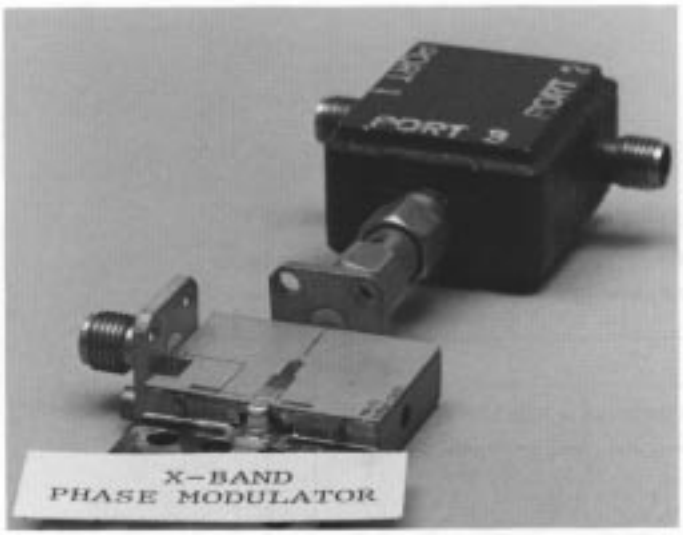

Fig. 5. X-band (8415 MHz) phase modulator.

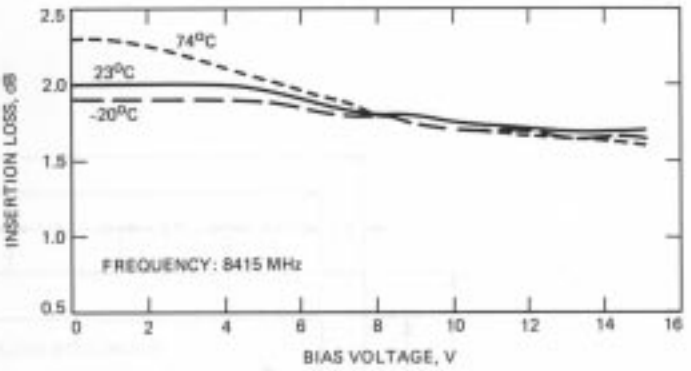

Fig. 8. Measured insertion loss versus dc bias voltage and temperature.

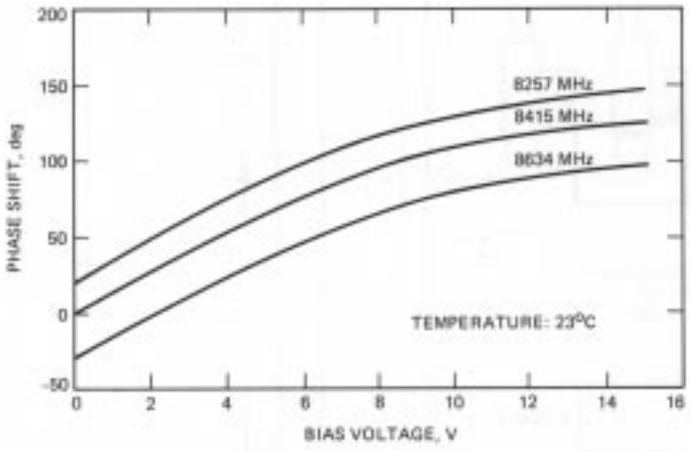

Fig. 6. Measured phase shift as a function of dc bias voltage and frequency.

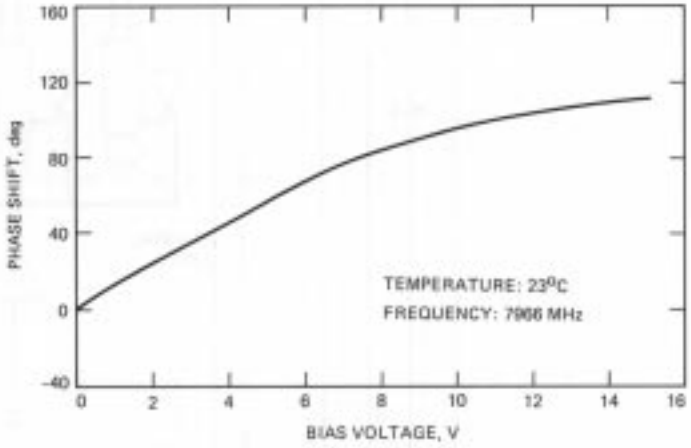

Fig. 9. Measured phase shift versus dc bias voltage.

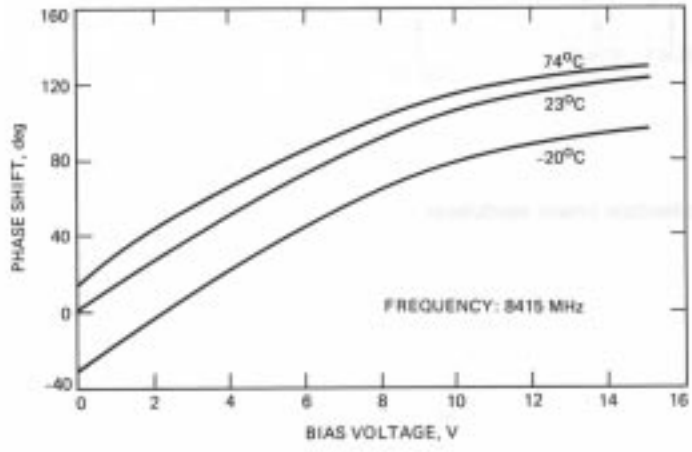

Fig. 7. Measured phase shift versus dc bias voltage and temperature.

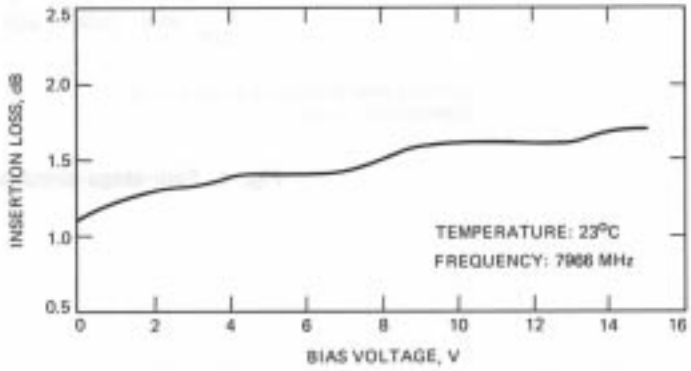

Fig. 10. Measured insertion loss versus dc bias voltage.